9-8-2022

Microgrid Energy Management during High-Stress Operation

Thomas Price
Michigan Technological University

Gordon Parker
Michigan Technological University, ggparker@mtu.edu

Gail Vaucher
U.S. Army Research Laboratory

Robert Jane
U.S. Army Research Laboratory

Morris Berman
U.S. Army Research Laboratory

energies

MDPI

Article

Microgrid Energy Management during High-Stress Operation

Thomas Price [1,†], Gordon Parker [1,†,*], Gail Vaucher [2], Robert Jane [3] and Morris Berman [3]

[1] Mechanical Engineering-Engineering Mechanics Department, Michigan Technological University, Houghton, MI 49931, USA
[2] US Army Research Laboratory, US Army Combat Capabilities Development Command, US Army Futures Command, White Sands Missile Range, NM 88002, USA
[3] US Army Research Laboratory, US Army Combat Capabilities Development Command, US Army Futures Command, Adelphi, MD 20783, USA
* Correspondence: ggparker@mtu.edu
† These authors contributed equally to this work.

Abstract: We consider the energy management of an isolated microgrid powered by photovoltaics (PV) and fuel-based generation with limited energy storage. The grid may need to shed load or energy when operating in stressed conditions, such as when nighttime electrical loads occur or if there is little energy storage capacity. An energy management system (EMS) can prevent load and energy shedding during stress conditions while minimizing fuel consumption. This is important when the loads are high priority and fuel is in short supply, such as in disaster relief and military applications. One example is a low-power, provisional microgrid deployed temporarily to service communication loads immediately after an earthquake. Due to changing circumstances, the power grid may be required to service additional loads for which its storage and generation were not originally designed. An EMS that uses forecasted load and generation has the potential to extend the operation, enhancing the relief objectives. Our focus was to explore how using forecasted loads and PV generation impacts energy management strategy performance. A microgrid EMS was developed exploiting PV and load forecasts to meet electrical loads, harvest all available PV, manage storage and minimize fuel consumption. It used a Model Predictive Control (MPC) approach with the instantaneous grid storage state as feedback to compensate for forecasting errors. Four scenarios were simulated, spanning a stressed and unstressed grid operation. The MPC approach was compared to a rule-based EMS that did not use load and PV forecasting. Both algorithms updated the generator's power setpoint every 15 min, where the grid's storage was used as a slack asset. While both methods had similar performance under unstressed conditions, the MPC EMS showed gains in storage management and load shedding when the microgrid was stressed. When the initial storage was low, the rule-based EMS could not meet the load requirements and shed 16% of the day's electrical load. In contrast, the forecast-based EMS managed the load requirements for this scenario without shedding load or energy. The EMS sensitivity to forecast error was also examined by introducing load and PV generation uncertainty. The MPC strategy successfully corrected the errors through storage management. Since weather affects both PV energy generation and many types of electrical loads, this work suggests that weather forecasting advances can improve remote microgrid performance in terms of fuel consumption, load satisfaction, and energy storage requirements.

Keywords: clear sky; electrical load forecast; fuel consumption; energy management system; energy storage requirements; microgrid; model predictive control; overcast sky; weather effects; weather forecast

Citation: Price, T.; Parker, G.; Vaucher, G.; Jane, R.; Berman, M. Microgrid Energy Management during High-Stress Operation. *Energies* **2022**, *15*, 6589. https://doi.org/10.3390/en15186589

Academic Editor: Giovanni Tinè

Received: 8 August 2022
Accepted: 5 September 2022
Published: 8 September 2022

1. Introduction

A microgrid is an electrical network containing one or more power sources, loads, and energy storage, interconnected with well-defined boundaries. It can be connected to a primary grid through a point of common coupling (PCC); otherwise, it is considered

an island [1–3]. Provisional microgrids used to meet temporary power requirements for disaster relief and military applications are typically islanded [4]. Low weight and fuel-efficient operations are essential features due to the difficulty in getting equipment and fuel to remote locations [5–7].

An islanded microgrid has low inertia, meaning its load can change rapidly compared to its generation capacity and energy storage. This leads to an increase in the probability of load loss [3]. Load forecasting has observed widespread implementation to improve microgrid performance [8–11]. Both islanded and connected microgrids exploit load forecasting to decrease the risk of load loss and improve storage management, enabling the full use of renewable resources.

While incorporating renewable sources into a microgrid is attractive, their inconsistent power generation creates an added dependence on storage requirements. Consequently, they serve best when blended with a variety of power sources. This raises a microgrid's cost and weight and is essential for provisional microgrid designs. As renewable energy penetration increases, generation forecasting becomes as crucial as load forecasting for efficient operation [12]. Photovoltaic (PV) power prediction relies on future panel temperature, and irradiance estimates [13]. Thus, weather forecasts play a significant role in PV power predictions [8,14]. Extending these methods to provisional microgrids is problematic since access to regional weather forecasts cannot be assumed to exist [15]. Alternate forms of PV forecast generation have been suggested, such as analyzing the sky conditions to generate forecasts of ambient temperature and irradiance [16,17]. Regional weather forecasts affect electrical load forecasts when heating and cooling equipment dominate.

A microgrid's EMS controls its assets, such as non-renewable generation and energy storage, to meet load requirements while minimizing cost, fuel, or an acoustic signature [18–20]. Zafeiropoulou et al. [21] describes an architecture where the relationship between historical meteorological and energy consumption data is used in several ways to improve power system performance. For example, machine learning schemes are used to predict the probability of outages or equipment damage when violent weather is predicted. This permits preemptive reconfiguration of assets to reduce the actual impact of weather events. The EMS described in the work below is similar in its dependence on load and meterological predictions of PV generation. A key difference is that our focus is on completely islanded, provisional microgrids and how forecasts can be used to service loads that occur at inconvenient times while helping to reduce energy storage requirements.

Kreishan describes the effects of unexpected islanding on mixed distributed energy resource (DER) systems. In addition, they develop and assess a method of planned islanding that mitigates the negative effects of this phenomenon [22]. They demonstrate their approach using a detailed model of a medium voltage power grid along with several resource islanding scenarios. One of the main benefits of their approach is the ability to service high priority loads. This is similar to the focus of the work below, where loads occurring an inconvenient times, such as at night, can be met with suitable planning. Unexpected islanding was also addressed by Worku et al. with the development of methods to detect islanding using the states of any microgrid attached to a primary power grid. [23]. Their grid architecture, and application of power flow analysis, is similar to the work presented below. One of the differences is that our microgrid is always islanded and its storage state information is used to adjust asset use to minimize fuel consumption.

Prodan and Zio consider the electricity price from an external grid to reduce renewable resource drawbacks [24]. An EMS can use both load and atmospheric forecasts to manage storage. This advantage allows loads to be met when renewable resources are offline and avoids shedding energy should the storage reach maximum capacity.

The EMS considered in this paper is motivated by low-power, provisional microgrid applications with no option to connect to a main grid. The notional grid used to compare EMS strategies, has a fuel-based generator with a maximum output of 100 W and electrical loads of less than 300 W. A PV panel also supplies the grid with a maximum output of 300 W. It should be noted that the EMS described here is not limited to a particular

generation of technology, renewable or otherwise. For example, a caloric-based generator could be used where an operator produces power through physical activity. Reducing battery requirements is imperative for such person-carried power systems, as it does not have the main grid as a backup, such as many other microgrid studies.

The primary focus is the effect of load and PV generation forecasts on the islanded power grid's performance. Two EMS strategies are developed and compared: one uses 24-h load and PV estimates, while the other only has access to the grid's current storage state, PV output, and load. Both algorithms provide a power setpoint command to the grid's generator every 15 min. Storage, if available, is used as a slack asset to balance the electrical load. The forecast-based EMS is implemented as a model predictive control (MPC) system, where the feedback is the grid's storage state of charge, and the cost function is the fuel consumption. The other algorithm is rule-based and seeks to reduce fuel consumption by ensuring the generator is continuously operating at peak efficiency. A power flow simulation is used to evaluate the performance of the two algorithms in terms of load satisfaction, storage requirements, and fuel consumption over a period of 24 h.

The remainder of this paper is organized as follows. After a description of the power flow grid model in Section 2, the forecast-based and rule-based EMS strategies are developed in Section 3. Four case studies are introduced in Section 4, followed by the results in Section 5 and conclusions in Section 6.

2. Grid Model

Not including storage, the net bus power, P_{net}, is defined as

$$P_{net} = P_{gen} + P_{PV} - P_{load} \tag{1}$$

where P_{gen} and P_{PV} are the generator and PV power into the electrical bus, and P_{load} is the electrical load power out of the bus. Energy storage power is used as a slack asset such that $P_{str} = P_{net}$ and its state of charge, E_{str}, is

$$E_{str} = E_0 + \int_0^t P_{net}\, dt, \quad 0 \leq E_{str} \leq E_{max} \tag{2}$$

where E_0 is the initial storage state and E_{str} is bounded from above by its capacity, E_{max}. It is further assumed that the storage is ideal and can increase and decrease its state instantaneously without loss. This means that as long as $0 \leq E_{str} \leq E_{max}$, the storage can match any value of P_{net} needed to satisfy the load. However, if $E_{str} = 0$ and $P_{net} < 0$, some of the electrical load must be shed, namely, $P_{load,shed} = -P_{net}$. The shed energy is given in Equation (3).

$$E_{load,shed} = -\int_0^t P_{net}\, dt, \quad E_{str} = 0, P_{net} \leq 0 \tag{3}$$

Similarly, when the storage is at capacity, $E_{str} = E_{max}$, and the electrical load is not perfectly balanced by the combined PV and generator power, bus energy must be shed, as shown in Equation (4).

$$E_{bus,shed} = \int_0^t P_{net}\, dt, \quad E_{str} = E_{max}, P_{net} \geq 0 \tag{4}$$

Regardless of its technology, a generator converts one form of energy to electrical energy with an assumed efficiency. It is assumed that the generator efficiency is defined in terms of a power-dependent fuel rate function, $\dot{m}_{fuel}(P_{gen})$ resulting in the fuel consumption, m_{fuel}, as shown in Equation (5).

$$m_{fuel} = \int_0^t \dot{m}_{fuel}(P_{gen})\, dt \tag{5}$$

The grid model can be summarized as having two states, E_{str} and m_{fuel}, calculated by Equation (2) and Equation (5), respectively. The shed bus energy and load of Equation (4) and Equation (3) will be used later to assess EMS performance.

3. Energy Management Systems

Two EMS strategies are developed below: (1) forecast-based and (2) rule-based. Both use grid state information to update the generator output command, with P_{gen} at a fixed time interval of T seconds.

3.1. Forecast-Based Solver

The forecast-based solver uses an MPC approach to create the generator command, P_{gen}, that is held until the next update, T, seconds later. The MPC algorithm uses the measured storage state, E_{str}, and estimates of both PV and load power, P_{PV} and P_{load}, over the horizon time T_h to compute a fuel optimal generator command sequence $\{P^*_{gen}\}$. The first element of this sequence is then used as the generator command until the next update. Since PV generation has a 24-h cycle, the horizon time should be at least 24 h. In the case studies considered later, $T_h = 24$ h and $T = 15$ min result in a 96 element generator command sequence. The MPC optimization problem used to calculate $P_{gen}(t_1)$ can be summarized as:

Given the grid's current energy state, $E_{str}(t_1)$, and estimates of $P_{PV}(t)$ and $P_{load}(t)$ where $t_1 \leq t < t_1 + T_h$, calculate P^*_{gen} that minimizes Equation (5) subject to the storage model of Equations (1) and (2), the inequality constraints

$$\begin{aligned} 0 < E_{str} < E_{max} \\ 0 < P_{gen} < P_{max} \end{aligned} \tag{6}$$

and the equality constraint

$$E_{str}(T_h) = E_0 \tag{7}$$

3.2. Rule-Based Solver

The rule-based EMS uses instantaneous measurements of P_{PV}, P_{load} and E_{str} to calculate a generator command, P_{gen}, that is held until the next update. The algorithm, shown in Figure 1, prioritizes storage use and attempts to operate the generator as little as possible, while maintaining the power balance of Equation (8). When the generator is in use, it is operated at max efficiency or $P_{gen} = P_{gen,max}$. The grid state measurements are used to create the three intermediate quantities, shown in Equation (9) and used in Figure 1.

$$P_{PV} + P_{str} + P_{gen} = P_{load} \tag{8}$$

$$\begin{aligned} P_{net} &= P_{load} - P_{PV} \\ P_{str} &= \frac{E_{str}}{T} \\ E_{str,max} &= E_{max} - E_{str} \end{aligned} \tag{9}$$

The algorithm can be summarized as follows. If $P_{net} \geq 0$, there is not enough PV to completely service the load, thus requiring a combination of generator and storage. The set of resulting subpaths is labeled A in the flow chart. If $P_{net} < 0$, labeled B in the flowchart, then the load can be serviced completely from the available PV and there is an opportunity to store excess PV energy.

Focusing on block A, there are three possible outcomes: (1) there exists sufficient storage to completely meet the load, labeled A_1, (2) the load must be met with a combination of storage and generation, labeled A_2, where the generator may operate at less than peak efficiency and (3) there is insufficient available energy, storage and load, and load must be shed. This worst case is labeled A_3.

The flowchart's block B has two paths based on the storage state. If there is enough excess capacity for all the additional PV energy, path B_2, then its stored. Otherwise, some of the excess energy must be shed, as shown in path B_1.

In summary, the five algorithm solutions are labeled at the bottom of the paths in Figure 1 as being either: good; inefficient, due to operating the generator at less than peak efficiency; or shedding either electrical load or PV energy.

After calculating P_{gen}, the secondary consideration of returning the storage state at the final time, $E_{str}(T_h)$, to its starting value of E_0, is considered. If the generator is not being used and $E_{str,new} < E_0$, then the generator is operated at full power as long as storage capacity exists.

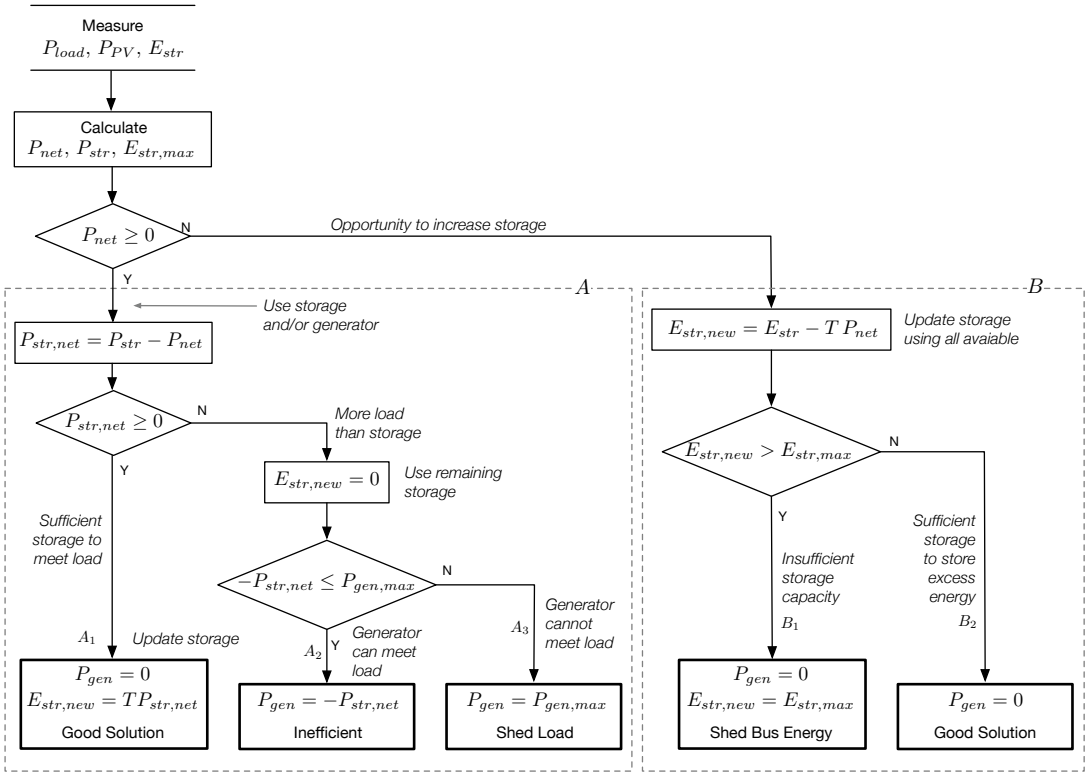

Figure 1. Flowchart of the rule-based EMS. The pathway blocks labeled A and B correspond to PV availability. Block A paths are used when there is not enough PV to meet the loads while the block B paths are used when there is enough PV to meet the loads and there is an opportunity to store excess energy.

4. Case Studies

Exploring the impact of using forecasted PV and load on EMS performance when operating in stressed conditions is a primary aim of this work. A small microgrid was considered with a 300 W PV panel and a 100 W generator, whose load-dependent efficiency function is shown in Figure 2. The generator consumes about 0.33 g of fuel per kJ of energy when operating at peak efficiency. The EMS is updated every 15 min, while a power flow simulation updates the grid states every second. It is assumed that a faster, inner loop maintains the bus voltage and is not part of this work. To emphasize the effect that accurate forecasts have on stressed operation, the load and PV forecasts are assumed to be exact at the start of each 15-min EMS update.

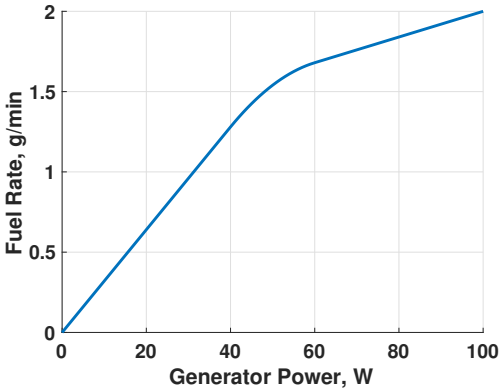

Figure 2. Fuel consumption rate as a function of power output for the 100 W generator.

Four cases are considered including a no-stress baseline, two stress scenarios and a situation where forecast errors are present. Each case is defined by a combination of electrical load, Figure 3a; a PV output based on one of two sky conditions, Figure 3b; and an energy storage configuration, including an initial storage state and two different capacities, Figure 3c. The 24-h load energy of 10,159 kJ is the same for all four cases to permit EMS performance comparisons between cases.

The baseline No Stress case uses a constant load of 118 W, as shown by the dashed line in Figure 3a. This is the least stressful situation, as it requires no load-change planning. The generated PV arises from a clear sky condition shown with a solid line in Figure 3b. This profile was measured using a PV panel on a cloudless day and has the classic Gaussian shape while generating 9332 kJ of energy. The energy storage conditions are shown with the first bar in Figure 3c where there is ample storage capacity, 14 MJ, and the day begins with the storage level at 7 MJ.

The two stress cases contain load changes - one occurring during the day when PV power is being generated and another at night shown by the dotted and solid lines in Figure 3a. Stress Case 1 has a step change in load from 86 W to 180 W lasting from 9 a.m. to 5 p.m. and requiring about 2707 kJ of energy. Since the load change occurs during daylight hours, this is considered to be less stressful than Stress Case 2 where the load change changes from 92 W to 300 W lasting from 8 p.m. to 11 p.m. The total energy required by the load pulse of Stress Case 2 is about 2250 W and is similar to Stress Case 1. The same PV generation profile for both stress cases is the measured value, as shown by the dotted line in Figure 3b that occurred during a day with overcast sky conditions. The energy generated was 2346 kJ, or about 25% of the No Stress, clear day. The storage scenarios for the stress cases are shown in Figure 3c, where Stress Case 1 has ample storage capacity, 14 MJ; however, the day starts with the storage at 13 MJ. This limits the ability of the EMS to store energy and could lead to energy shedding. The storage capacity of Stress Case 2 is much reduced, 3 MJ, and the day starts with 0.5 MJ of energy. This too is considered a stress situation where EMS planning must account for a highly constrained storage situation.

The forecast error case is a variant of Stress Case 2, where the night transient is increased by 10%, as shown by the blue lines in Figure 4, where the dotted line is the forecast and the solid line is the actual. The 24-h load energy, 10,159 kJ, is the same as the previous cases, thus the constant value before the night transient was reduced slightly. The 24-h PV energy is shown in Figure 4 by the black lines. The forecasted solid line contains both over and under predictions with the same amount of energy as the dotted, actual value. This was accomplished by reducing the first half and increasing the second half by adding two periods of a versine function with an amplitude of 50 W.

The four cases are summarized in Table 1 along with the minimum possible value of generator output and fuel consumption.

Table 1. Summary of the four cases used to evaluate the EMS strategies.

	No Stress	Stress Case 1	Stress Case 2	Forecast Error Case
Load, kJ	10,159	10,159	10,159	10,159
PV Output, kJ	9332	2346	2346	2346
Storage Capacity, E_{max}, MJ	14	14	3	14
Initial Storage, E_0, MJ	7	13	0.5	13
Minimum Generator Output, kJ	827	7813	7813	7813
Minimum Fuel Consumption, kg	0.27	2.58	2.58	2.58

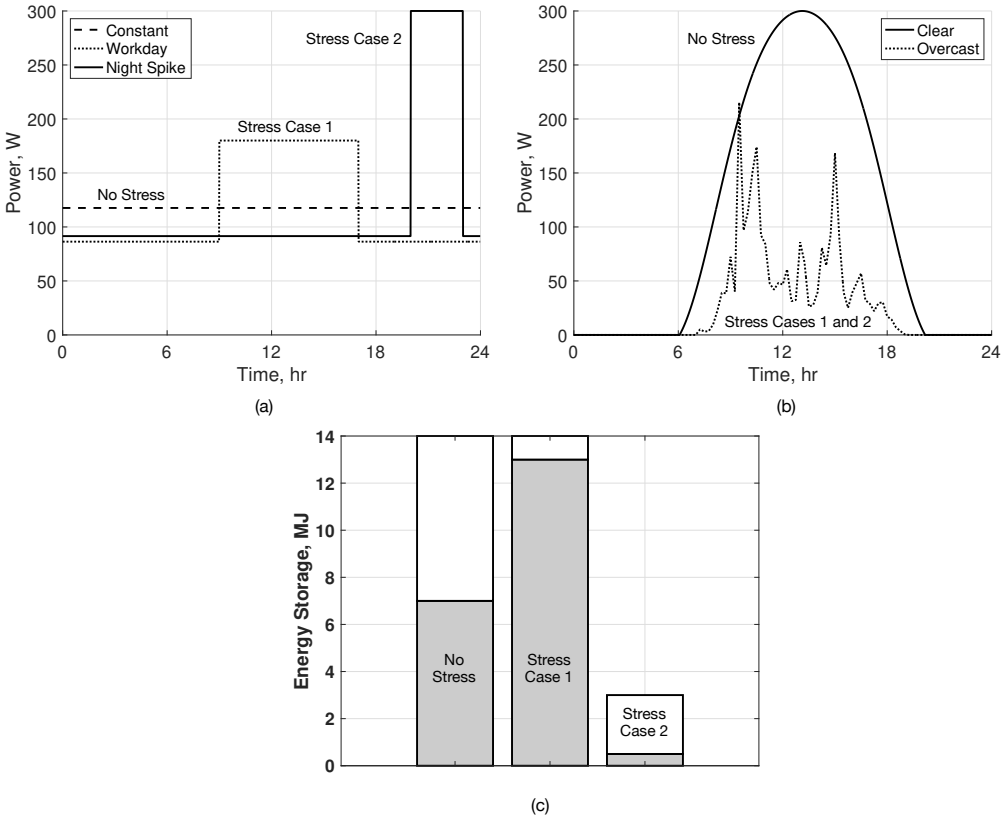

Figure 3. Electrical load, PV generation, and storage state cases used to create the three scenarios used in the case studies. The electrical loads (**a**) consume the same amount of energy, 10,159 kJ, in 24 h. The two PV generation scenarios, (**b**), are based on measured data for two extreme sky conditions: clear and overcast, producing 9332 kJ and 2346 kJ in 24 h. The energy storage bars, (**c**), show capacity, E_{max} and initial states, and E_0 for the three cases.

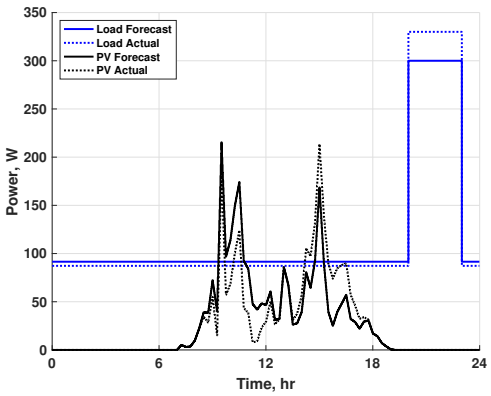

Figure 4. The electrical load and PV generation for the Forecast Error Case.

5. Results

The performance of the forecast-based and rule-based EMS, for the four cases described above, are summarized in Table 2 and plotted in Figures 5–8. Energy balance analysis can be performed using the table entries. For example, the sum of the PV Output, Generator Output, Net Storage Output and Shed Load is equal to the Load. It is important to note that a positive value of the Net Storage Output means that energy is being stored. The four figures contain identical information for each case. Subfigure (a) shows the load, PV, and generator power for forecast-based and rule-based strategies, while subfigure (b) shows the evolution of the stored energy. If the PV was utilized perfectly, the No Stress Case would have required 827 kJ from the generator, and the other cases needed 7813 kJ. Any deviation from these values implies some of the electrical load was shed, or the storage constraints were not met, as tabulated in the Net Storage Output row of Table 2, whose entries should ideally all be zero. The Fuel Use row is another indicator of optimal operation, with 0.27 kg being the best possible value for the No Stress Case and 2.58 kg for all the others. Examining Figures 5–8, it is clear that the generator was either off or at full load, corresponding to maximum efficiency. The Fuel Use row of Table 2 shows that the forecast-based EMS was operated nearly optimal for all cases without shedding any load, while the rule-based EMS struggled with storage management and load shedding for some of the cases.

The rule-based EMS consumed much more fuel than necessary while ending the day with 2234 kJ of excess energy for the No Stress case, as observed in Table 2 and Figure 5. This is not a problem; it simply means that the storage should be used before the generator begins the next day. However, if this behavior is repeated daily, it will become unsustainable. Both strategies performed the same for the second stress case, with the rule-based EMS having a slightly larger final storage error. This could be compensated as in the No Stress Case the next day.

The second stress case, where the PV was low and there was a load spike during the night, resulted in a significant difference between the strategies, as observed in Table 2 and Figure 7. The rule-based strategy needed to shed about 16% of the load with a corresponding reduction in fuel use. A similar load-shedding occurred for the Forecast Error Case, which is not surprising, since the PV and load conditions were similar. The forecast-based solver performed nearly the same for the Forecast Error Case as for Stress Case 2. This illustrates that while forecasts are exploited, the solver is also robust to forecast errors due to the storage feedback used in its model predictive controller.

Table 2. Comparison of the forecast-based and rule-based EMS performance for the four scenarios described above. Note: the theoretical optimal fuel consumption for the No Stress case is 0.27 kg and 2.58 kg for all the other cases.

	No Stress		**Stress Case 1**		**Stress Case 2**		**Forecast Error Case**	
EMS Method:	**Forecast**	**Rule**	**Forecast**	**Rule**	**Forecast**	**Rule**	**Forecast**	**Rule**
Load (kJ)	10,159	10,159	10,159	10,159	10,159	10,159	10,159	10,159
PV Output (kJ)	9332	9332	2346	2346	2346	2346	2346	2346
Generator Output (kJ)	900	3060	7830	7740	7830	5640	7650	5310
Net Storage Output (kJ)	−73	−2233	−17	73	−17	504	163	−459
Shed Load (kJ)	0	0	0	0	0	1669	0	2044
Fuel Use (kg)	0.30	1.01	2.58	2.55	2.58	1.86	2.52	1.75
Required Storage Capacity (kJ)	4547	4751	768	562	2499	n/a	2678	n/a
Required Initial Storage (kJ)	2806	400	73	538	149	n/a	204	n/a

We can also extract storage requirement information from Figures 5–8. For example, the minimum initial storage needed by either EMS is the difference between E_0 and the minimum storage state during the day. The minimum storage capacity is the difference between the minimum and maximum of the storage state plots. These are shown in Table 2,

where they are similar for the No Stress case and the first stress case. The rule-based values are not shown for the last two cases, since their meaning is obscured due to the load shedding. While the forecast-based solver could compensate for forecast errors, it required about 7% more storage capacity than the closely-related Stress Case 2 to manage the uncertainty.

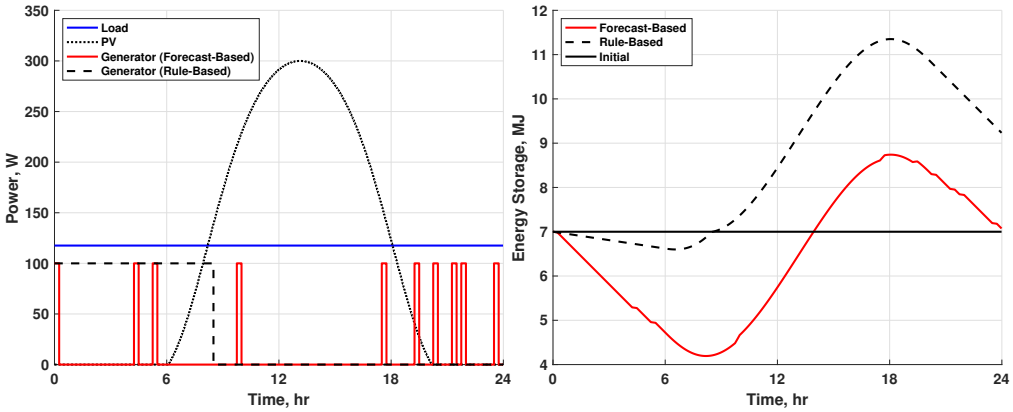

(a) **(b)**

Figure 5. No stress case power (**a**) and energy storage (**b**).

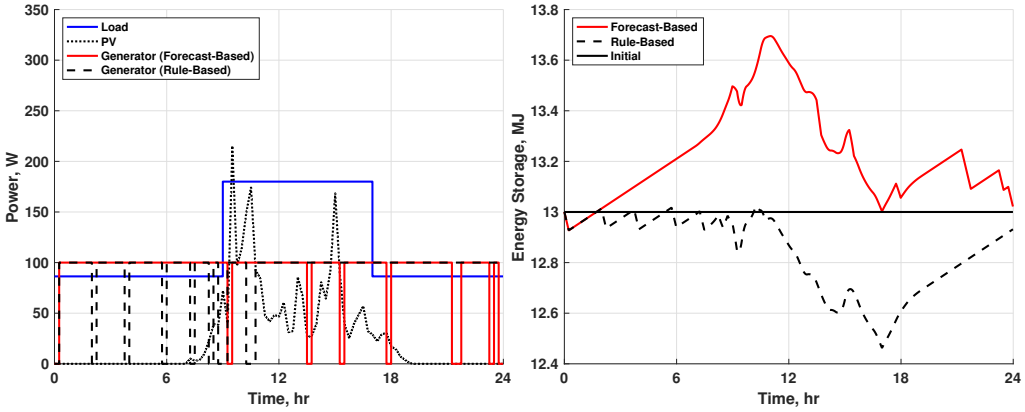

(a) **(b)**

Figure 6. Stress case 1 power (**a**) and energy storage (**b**).

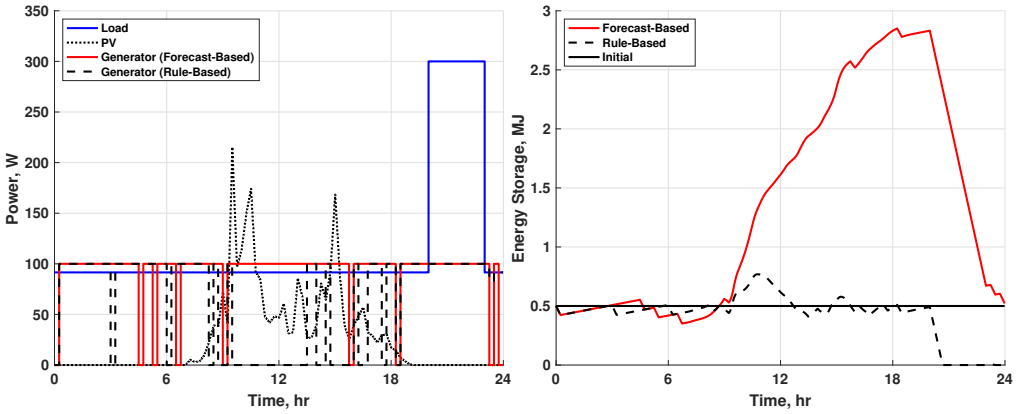

(a) **(b)**

Figure 7. Stress case 2 power (**a**) and energy storage (**b**).

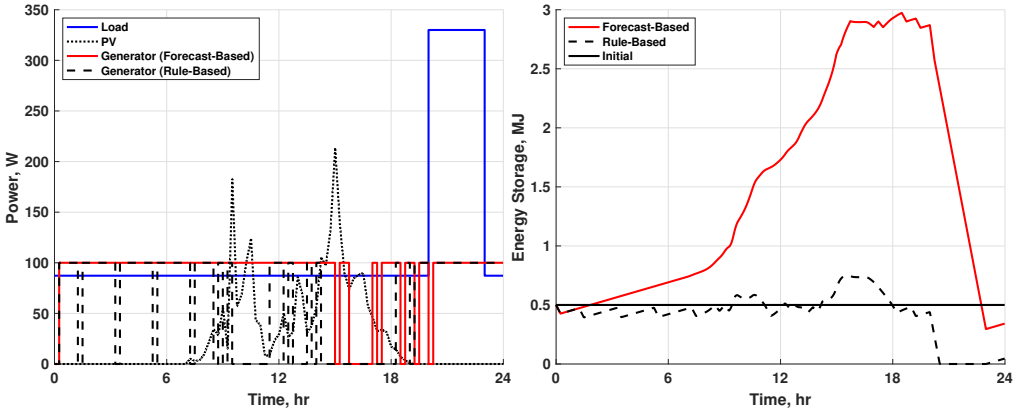

(a) **(b)**

Figure 8. Forecast error case power (**a**) and energy storage (**b**).

6. Conclusions

Both EMS methods performed similarly for clear and overcast sky conditions when the maximum electrical load occurred during the day. At the same time, the rule-based strategy could not return the final storage state to its starting value, which is not a significant issue as long as the storage is adjusted the next day and the behavior is not repeated too often. The computational effort of the rule-based approach is insignificant compared to the numerical optimization solver used for the forecast-based solver. The combined genetic algorithm and gradient-based scheme of the forecast-based EMS required about one minute to find a solution compared to a millisecond for the rule-based EMS. Since the rule-based solution performed well in some circumstances, it could be used as a backup solution for a single 15-min epoch should the optimization process fail or timeout during one of its solutions.

The second two cases, where a load spike occurred when the PV was unavailable, showed significant differences between the two methods. The rule-based strategy was required to shed some electrical load in both cases. In contrast, the forecast-based solver planned for the event by increasing the storage state in advance. While the forecast-based solver relies on forecasts of both PV and load, it can accommodate errors in both these quantities, as illustrated by the Forecast Error Case.

Author Contributions: The individual contributions of each of the four authors, T.P., G.P., G.V., R.J. and M.B. are as follows; Conceptualization, T.P. and G.P.; Data curation, T.P., G.P. and G.V.; Formal analysis, T.P. and G.P.; Funding acquisition, M.B.; Investigation, T.P., G.P., G.V., R.J. and M.B.; Methodology, T.P., G.P., G.V., R.J. and M.B.; Project administration, M.B.; Resources, G.V. and M.B.; Software, T.P., G.P. and R.J.; Supervision, G.P.; Validation, R.J. and G.P.; Visualization, R.J., G.P., G.V. and M.B.; Writing an original draft, T.P. and G.P.; Writing, reviewing and editing, T.P., G.P., G.V., R.J. and M.B. All authors have read and agreed to the published version of the manuscript.

Funding: This work was supported by the Army Futures Command Army Research Laboratory (ARL) under the contract CA W911NF-17-2-0130.

Institutional Review Board Statement: Not applicable.

Informed Consent Statement: Not applicable.

Data Availability Statement: Not applicable.

Conflicts of Interest: The authors declare no conflict of interest.

Disclaimer: Reference herein to any specific commercial company, product, process, or service by trade name, trademark, manufacturer, or otherwise, does not necessarily constitute or imply its endorsement, recommendation, or favoring by the United States Government or the Department of the Army (DoA). The opinions of the authors expressed herein do not necessarily state or reflect those of the United State Government of the DoA, and shall not be used for advertising or product endorsement purposes.

References

1. Lasseter, R.H. Microgrids. In Proceedings of the 2002 IEEE Power Engineering Society Winter Meeting. In Proceedings of the Conference Proceedings (Cat. No.02CH37309), New York, NY, USA, 27–31 January 2002; Volume 1, pp. 305–308.
2. Katiraei, F.; Iravani, M.R.; Lehn, P.W. Micro-grid autonomous operation during and subsequent to islanding process. *IEEE Trans. Power Deliv.* **2005**, *20*, 248–257. [CrossRef]
3. Olivares, D.E.; Mehrizi-Sani, A.; Etemadi, A.H.; Cañizares, C.A.; Iravani, R.; Kazerani, M.; Hajimiragha, A.H.; Gomis-Bellmunt, O. Trends in Microgrid Control. *IEEE Trans. Smart Grid* **2014**, *5*, 1905-1919. [CrossRef]
4. Mitra, J.; Vallem, M.R. Determination of storage required to meet reliability guarantees on island-capable microgrids with intermittent sources. *IEEE Trans. Power Syst.* **2012**, *27*, 2360–2367. [CrossRef]
5. Kashem, S.B.A.; De Souza, S.; Iqbal, A.; Ahmed, J. Microgrid in military applications. In Proceedings of the 2018 IEEE 12th International Conference on Compatibility, Power Electronics and Power Engineering (CPE-POWERENG 2018), Doha, Qatar, 10–12 April 2018; pp. 1–5.
6. Peterson, C.J.; Van Bossuyt, D.L.; Giachetti, R.E.; Oriti, G. Analyzing mission impact of military installations microgrid for resilience. *Systems* **2021**, *9*, 69. [CrossRef]
7. Peerapong, P.; Limmeechokchai, B. Optimal electricity development by increasing solar resources in diesel-based micro grid of island society in Thailand. *Energy Rep.* **2017**, *3*, 1–13. [CrossRef]
8. Parhizi, S.; Lotfi, H.; Khodaei, A.; Bahramirad, S. State of the Art in Research on Microgrids: A Review. *IEEE Access* **2015**, *3*, 890–925. [CrossRef]
9. Moradzadeh, A.; Zakeri, S.; Shoaran, M.; Mohammadi-Ivatloo, B.; Mohammadi, F. Short-term load forecasting of microgrid via hybrid support vector regression and long short-term memory algorithms. *Sustainability* **2020**, *12*, 7076. [CrossRef]
10. Liu, N.; Tang, Q.; Zhang, J.; Fan, W.; Liu, J. A hybrid forecasting model with parameter optimization for short-term load forecasting of micro-grids. *Appl. Energy* **2014**, *129*, 336–345. [CrossRef]
11. Hernandez, L.; Baladrón, C.; Aguiar, J.M.; Carro, B.; Sanchez-Esguevillas, A.J.; Lloret, J. Short-term load forecasting for microgrids based on artificial neural networks. *Energies* **2013**, *6*, 1385–1408. [CrossRef]
12. Rahbar, K.; Xu, J.; Zhang, R. Real-time energy storage management for renewable integration in microgrid: An off-line optimization approach. *IEEE Trans. Smart Grid* **2014**, *6*, 124–134. [CrossRef]
13. Diagne, M.; David, M.; Lauret, P.; Boland, J.; Schmutz, N. Review of solar irradiance forecasting methods and a proposition for small-scale insular grids. *Renew. Sustain. Energy Rev.* **2013**, *27*, 65–76. [CrossRef]
14. Massucco, S.; Mosaico, G.; Saviozzi, M.; Silvestro, F. A hybrid technique for day-ahead PV generation forecasting using clear-sky models or ensemble of artificial neural networks according to a decision tree approach. *Energies* **2019**, *12*, 1298. [CrossRef]
15. Agüera-Pérez, A.; Palomares-Salas, J.C.; de la Rosa, J.J.G.; Florencias-Oliveros, O. Weather forecasts for microgrid energy management: Review, discussion and recommendations. *Appl. Energy* **2018**, *228*, 265–278. [CrossRef]
16. Jane, R.; Parker, G.; Vaucher, G.; Berman, M. Characterizing Meteorological Forecast Impact on Microgrid Optimization Performance and Design. *Energies* **2019**, *13*, 577. [CrossRef]
17. Zhen, Z.; Liu, J.; Zhang, Z.; Wang, F.; Chai, H.; Yu, Y.; Lu, X.; Wang, T.; Lin, Y. Deep learning based surface irradiance mapping model for solar PV power forecasting using sky image. *IEEE Trans. Ind. Appl.* **2020**, *56*, 3385–3396. [CrossRef]
18. Anglani, N.; Oriti, G.; Colombini, M. Optimized energy management system to reduce fuel consumption in remote military microgrids. *IEEE Trans. Ind. Appl.* **2017**, *53*, 5777–5785. [CrossRef]
19. Mendes, P.R.; Isorna, L.V.; Bordons, C.; Normey-Rico, J.E. Energy management of an experimental microgrid coupled to a V2G system. *J. Power Sources* **2016**, *327*, 702–713. [CrossRef]
20. Kaur, A.; Kaushal, J.; Basak, P. A review on microgrid central controller. *Renew. Sustain. Energy Rev.* **2016**, *55*, 338–345. [CrossRef]
21. Zafeiropoulou, M.; Mentis, I.; Sijakovic, N.; Terzic, A.; Fotis, G.; Maris, T.I.; Vita, V.; Zoulias, E.; Ristic, V.; Ekonomou, L. Forecasting Transmission and Distribution System Flexibility Needs for Severe Weather Condition Resilience and Outage Management. *Appl. Sci.* **2022**, *12*, 7334. [CrossRef]
22. Kreishan, M.Z.; Fotis, G.P.; Vita, V.; Ekonomou, L. Distributed Generation Islanding Effect on Distribution Networks and End User Loads Using the Load Sharing Islanding Method. *Energies* **2016**, *9*, 956. [CrossRef]
23. Worku, M.Y.; Hassan, M.A.; Maraaba, L.S.; Abido, M.A. Islanding Detection Methods for Microgrids: A Comprehensive Review. *Mathematics* **2021**, *9*, 3174. [CrossRef]
24. Prodan, I.; Zio, E. A model predictive control framework for reliable microgrid energy management. *Int. J. Electr. Power Energy Syst.* **2014**, *61*, 399–409. [CrossRef]